Construction of CoP/Co$_2$P Coexisting Bifunctional Self-Supporting Electrocatalysts for High-Efficiency Oxygen Evolution and Hydrogen Evolution

Linyi Zhang, Yu Chen, Guangsheng Liu, Zhen Li, Song Liu, Santosh K. Tiwari, Oluwafunmilola Ola, Bingyan Pang, Nannan Wang,* and Yanqiu Zhu

| ACCESS | | Metrics & More | | Article Recommendations | | Supporting Information |
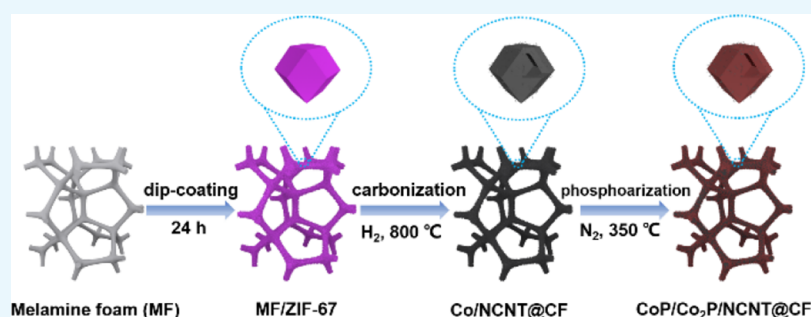
ABSTRACT: Development of a low cost, high activity, and stable nonprecious metal bifunctional catalyst for electrocatalytic water cracking is a hot topic and big challenge. In this paper, we prepared a nitrogen-doped carbon nanotube (NCNT)-enhanced three-dimensional self-supported electrocatalyst with CoP and Co$_2$P coexistence by a two-step strategy of high-temperature carbonization and low-temperature phosphorylation. Furthermore, the induced three-dimensional carbon network skeleton facilitates rapid charge transfer. In addition, the active sites of the carbon foam (CF) are greatly increased by the construction of hollow structures. As a bifunctional electrocatalyst, CoP/Co$_2$P/NCNT@CF exhibited excellent catalytic activity for both hydrogen evolution reaction and oxygen evolution reaction in alkaline media, requiring low overpotentials of 133 and 289 mV to obtain a current density of 10 mA cm^{-2}, respectively. Additionally, the synthesized catalysts also exhibit good long-term stability, maintaining high catalytic activity after 20 h of continuous operation. We also confirmed the main driving force to improve the electron transfer between the heterostructures of Co and P by XPS spectra. The excellent electrocatalytic performance can be attributed to the close synergy between the highly active CoP/Co$_2$P/NCNT and CF. This study provides a new strategy for the design of highly active bifunctional self-supporting electrocatalysts.

1. INTRODUCTION

Developing renewable clean energy that can replace traditional fossil energy can not only solve the global energy crisis but also contribute to environmental protection, which is also the direction that researchers have been working on for a long time. Hydrogen energy is considered to be the most efficient clean energy source of the 21st century due to its high combustion calorific value, nonpolluting nature, abundant sources, and sustainability, which attracts increasing attention from scientific researchers.[1,2] Electrocatalytic water cracking is a promising solution for the sustainable production of hydrogen and zero carbon emission throughout the process.[3] Electrocatalytic water cracking is divided into two half-reactions: the cathodic hydrogen evolution reaction (HER) and the anodic oxygen evolution reaction (OER).[4] The theoretical voltage of water cracking is 1.23 V.[5] However, in practical working conditions, especially in alkaline environments, a larger overpotential is often required to overcome the

reaction energy barrier to achieve water cracking.[6] Noble metal platinum (Pt)-based nanocomposites are currently excellent electrocatalysts for HER, while RuO$_2$ and IrO$_2$ are usually the most efficient electrocatalysts for OER.[7,8] However, the large-scale application of these noble metal-based electrocatalysts in industrial production has been hindered due to their scarce resources, high cost, and poor stability.[9] Therefore, in line with the principle of cost reduction and resource saving, it is essential to design an efficient and stable dual-function electrocatalyst with both HER and OER catalytic activities.

In recent years, transition metal-based materials have attracted much attention due to their abundant resources, low cost, and excellent electrocatalytic activity.[10] The flexible electronic structure of Co makes it stand out from the many transition metals as a promising raw material for the synthesis of highly efficient hydrolysis catalysts.[11] A great deal of research has been devoted to the development of cobalt-based compounds with good electrocatalytic capabilities. Common cobalt-based compounds include cobalt-based oxides,[12,13] hydroxides,[14] sulfides,[15,16] phosphides,[17−19] carbides,[20,21] nitrides,[22] etc. Among them, transition metal phosphides have a similar structure to hydrogenases, making cobalt phosphides of great potential for catalytic HER.[23] In recent years, an increasing number of studies have found that transition metal phosphides also contribute to catalyzing OER. For instance, Zhang et al. transformed one-dimensional Co_3O_4 nanowire into porous CoP nanowire through the anion exchange reaction; the CoP PNWs serve as bifunctional electrocatalysts, achieving a current density of 10 mA cm^{-2} with low overpotentials of 147 and 326 mV for HER and OER, respectively.[24] Although various cobalt phosphide electrocatalysts have been reported, there is still much room for development of bifunctional catalysts for simultaneous enhancement of HER and OER performance. The electrocatalytic performance can generally be improved by improving the electrical conductivity of the material and increasing the number of active sites in the catalyst. The conductivity and stability of the catalyst can be improved by using carbon material coating or loading, so as to improve its catalytic performance. The use of various carbon materials, such as graphene,[25] carbon nanotubes,[26,27] carbon paper,[28] carbon cloth,[29] and carbon fibers,[30] as catalyst carriers has been reported in the literature. For example, Xie et al.[31] developed a CoP/CNF bifunctional catalyst by in situ growth of CoP nanosheets on the CNF substrate. The synergetic effect of two-dimensional CoP nanosheets and one-dimensional CNFs endowed the CoP/CNF composites with abundant active sites and rapid electron transport pathways and thereby significantly improved the electrocatalytic performances. To improve bifunctional catalytic performance, it is often possible to construct heterogeneous structures[32,33] in which synergistic effects occur between different components, resulting in the formation of multiple active centers.[34] It has been pointed out that CoP contains abundant Co−P bonds favoring HER, while the large amount of Co−Co bonds in Co_2P favors the formation of OER active intermediates (OOH*).[35] CoP/Co_2P can enhance HER and OER performance through synergistic effects, so the combination of different cobalt phosphides may be an effective way to promote electrocatalytic hydrolysis. In addition, heteroatomic doping,[36] nanostructure, and porous structure can be used to expose more catalytic active sites and improve catalytic performance.

Metal−organic frameworks (MOF) are a kind of three-dimensional porous crystal material formed by the self-assembly of metal ions and organic ligands.[37] They are characterized by high porosity, large specific surface area, tunable structure, and good physicochemical stability.[8] Zeolite imidazole frameworks (ZIFs) are a subclass of the MOF family and have attracted the attention of many researchers in the fields of adsorption, separation, catalysis, and drug delivery.[38−41] In addition to the advantages of MOF materials mentioned above, ZIF materials contain large amounts of C and N elements, of which nitrogen can be used as a heteroatom to form nitrogen-doped carbon materials that serve as excellent precursors for electrocatalysts.[42] Pan et al. reported a hybrid nanostructure derived via core−shell ZIF-8@ZIF-67, where CoP nanoparticles were embedded in N-doped carbon nanotubes, exhibiting excellent electrocatalytic properties.[43] However, metal-containing nanocarbon electrocatalysts derived from MOFs/ZIFs usually require polymers such as Nafion/PVDF as binders when designed as electrodes, yet the use of binders not only clogs the active center but also reduces the electrical conductivity and hence the catalytic activity of the catalyst.[44] To address these issues, finding a suitable conductive substrate to combine with MOF/ZIF-derived nanomaterials as a self-supporting electrode is a feasible strategy. Based on the above considerations and with the principle of resource conservation, we have chosen low-cost melamine foam (MF) as the substrate for the loaded catalyst to prepare a zero-binder self-supporting electrocatalyst. MF has a three-dimensional interconnected porous network structure. Moreover, it is rich in surface functional groups and a large amount of carbon and nitrogen. After high-temperature carbonization, the three-dimensional carbon foam still retains the porous network structure perfectly and has electrical conductivity, so it is an ideal substrate for the preparation of an efficient electrocatalyst.

In this work, we report a reliable, low-cost, and scalable method to prepare a novel three-dimensional electrocatalyst. ZIF-67 was grown in situ on the MF skeleton, and nitrogen-doped CNT-enhanced three-dimensional hollow CoP/Co_2P/NCNT@CF was obtained through two steps of high-temperature carbonization and low-temperature phosphorylation. The porous network structure of the MF skeleton is conducive to the desorption of precipitated gas during the reaction process. The experimental results show that it can be used as a bifunctional electrocatalyst of HER and OER for water cracking. In 1 M KOH, CoP/Co_2P/NCNT@CF only requires low overpotentials of 133 and 289 mV to drive a current density of 10 mA cm^{-2} for HER and OER, respectively. The catalyst also has good durability in alkaline electrolytes. Our work provides a new idea for the development of nonprecious metal bifunctional self-supporting electrode materials.

2. EXPERIMENTAL SECTION

2.1. Materials. MF is provided by Xuxian Industrial (Shanghai) Co., Ltd. $Co(NO_3)_2 \cdot 6H_2O$, methanol, and KOH were purchased from Guangdong Guanghua Sci-Tech Co., Ltd. 2-Methylimidazole and $NaH_2PO_2 \cdot H_2O$ were purchased from Shanghai Aladdin Biochemical Technology Co., Ltd. Deionized water used in the experiment was made from ultrapure water in the lab. All the chemicals used in this experiment are analytical pure grade and need no further purification.

2.2. Synthesis of the Co/NCNT@CF Composite. MF (4 cm × 4 cm × 4 cm) was ultrasonically cleaned with ethanol and deionized water for 5 min and then dried in an oven at 60 °C for 24 h. Next, 0.015 mol $Co(NO_3)_2 \cdot 6H_2O$ and 0.06 mol 2-methylimidazole were dissolved in 300 mL of MeOH to form two clarified solutions, and then, the 2-MeIm solution was quickly poured into the $Co(NO_3)_2 \cdot 6H_2O$ solution and stirred for 5 min. The clean MF was immersed in the above purple mixture and continuously stirred for 1 h. In order to fully impregnate the interior of the MF cubes with the solution, a 2 h vacuum venting process is carried out, followed by aging at
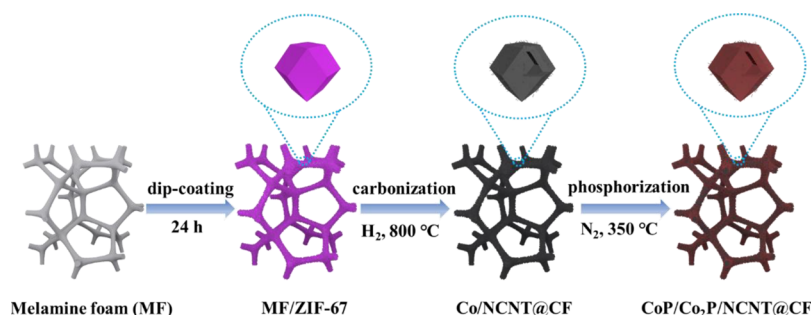
Figure 1. Schematic illustration of the synthesis process of CoP/Co$_2$P/NCNT@CF.

room temperature for 24 h. At the end of the resting period, 75% pressure was applied to the purple MF cubes to remove excess solution from the foam pores. The purple MF cubes were rotated and dried on a self-made rotator for 24 h to prevent uneven distribution of the ZIF-67 adsorbed in the MF due to the gravity effect. After this, the purple MF cube was placed in a vacuum drying oven at 80 °C to continue drying. The dried samples were placed in a tube furnace under an H$_2$/Ar (10%/90% in volume ratio) atmosphere, slowly ramped up to 350 °C, and held for 1.5 h, followed by a slow ramp up to 800 °C for 3.5 h to obtain Co/NCNT@CF.

2.3. Synthesis of the CoP/Co$_2$P/NCNT@CF Composite. A piece of synthesized Co/NCNT@CF was placed on one end of the porcelain boat, and a certain amount of NaH$_2$PO$_2$·H$_2$O was weighed as the phosphorus source according to a mass ratio of 1:10 and placed on the other end of the porcelain boat. The porcelain boat was placed in a tube furnace with the phosphorus source end on the upstream side and the sample end on the downstream side. The temperature was slowly ramped to 350 °C under an N$_2$ atmosphere and held for 2 h to obtain CoP/Co$_2$P/NCNT@CF.

For comparison, MF was carbonized directly under an argon atmosphere at 800 °C to obtain a carbon foam, denoted as CF.

2.4. Characterization and Electrochemical Measurement. The crystal structure of the samples was characterized by powder X-ray diffraction (XRD, SMARTLAB, Tokyo, Japan) with Cu Kα radiation (λ = 1.5418 Å). The morphology and the lattice spacing of the samples were obtained using a field emission scanning electron microscope (FE-SEM, ZEISS Sigma 300, Germany) equipped with an X-ray energy-dispersive spectrometer (EDS) and high-resolution transmission electron microscope (HRTEM, Tecnai G2 F30, Oregan, USA). The elemental microanalysis and atom binding states were examined by X-ray photoelectron spectroscopy (XPS, ESCALAB 250XI, Waltham, USA) with an Al Kα radiator.

All electrochemical measurements were carried out using an electrochemical workstation (CHI 660E, ChenHua Instruments Co. Ltd., Shanghai, China) with a typical three-electrode setup. A catalyst sample of 1 × 1 cm and 1 mm thick (mass loading ~3 mg cm^{-2}) was cut and sandwiched between two pieces of nickel foam of the same size to act as a working electrode. Pt/C and RuO$_2$ were made into traditional catalyst ink and coated on foam nickel to prepare working electrodes, and the load was controlled at 3~4 mg. Hg/HgO and the carbon rod served as the reference electrode and counter electrode, respectively. Linear sweep voltammetry (LSV) was used to obtain polarization curves at a scanning rate of 5 mV s^{-1} to evaluate the electrocatalytic activity of the samples. Electrochemical impedance spectroscopy (EIS) was performed

at various overpotentials with frequency from 0.1 to 100,000 Hz. To evaluate the electrochemical active surface area of the catalysts, the double-layer capacitances (C_{dl}) were measured by cyclic voltammetry (CV). EIS data were analyzed and fitted with the software of Zview. The stability of the catalyst was continuously tested by chronograph amperometry for 20 h. The HER performance was tested in 1 M KOH (pH = 14) solution. All potentials were calibrated to a reversible hydrogen electrode $E(RHE)$: $E(RHE) = E(Hg/HgO) + E^{\theta} + 0.059*pH$ ($E^{\theta} = 0.098$ in 1 M KOH). All the ohmic potential drop caused by solution resistance has been corrected with 90% iR-correction.

3. RESULTS AND DISCUSSION

3.1. Morphological and Structure Characterization. Figure 1 illustrates the synthesis process of the hollow polyhedron CoP/Co$_2$P/NCNT@CF on the MF skeleton. In brief, the white MF was dipped into the purple mixture, and the MF skeleton was evenly impregnated with a layer of ZIF-67 particles to obtain the purple MF/ZIF-67 cube. The MF/ZIF-67 cubes were carbonized at 800 °C under a hydrogen atmosphere to give Co/NCNT@CF and subsequently phosphated at 350 °C to give three-dimensional hollow CoP/Co$_2$P/NCNT@CF. Its digital photograph is shown in Figure S1.

The crystal structures of the sample were characterized by XRD, and the results are shown in Figure 2 The XRD pattern of Co/NCNT@CF shows three diffraction peaks at 44.2°, 51.5°, and 75.8°, corresponding to the (111), (200), and (220) crystal planes of metallic Co (JCPDS No. 15-0806), respectively. The characteristic peaks at 31.6°, 35.3°, 36.3°,
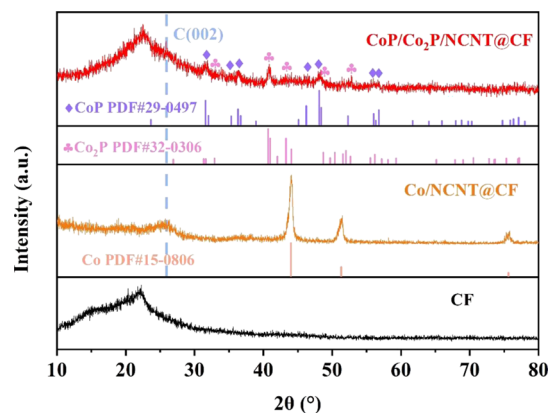
Figure 2. XRD patterns of CoP/Co$_2$P/NCNT@CF, Co/NCNT@CF, and pure CF.
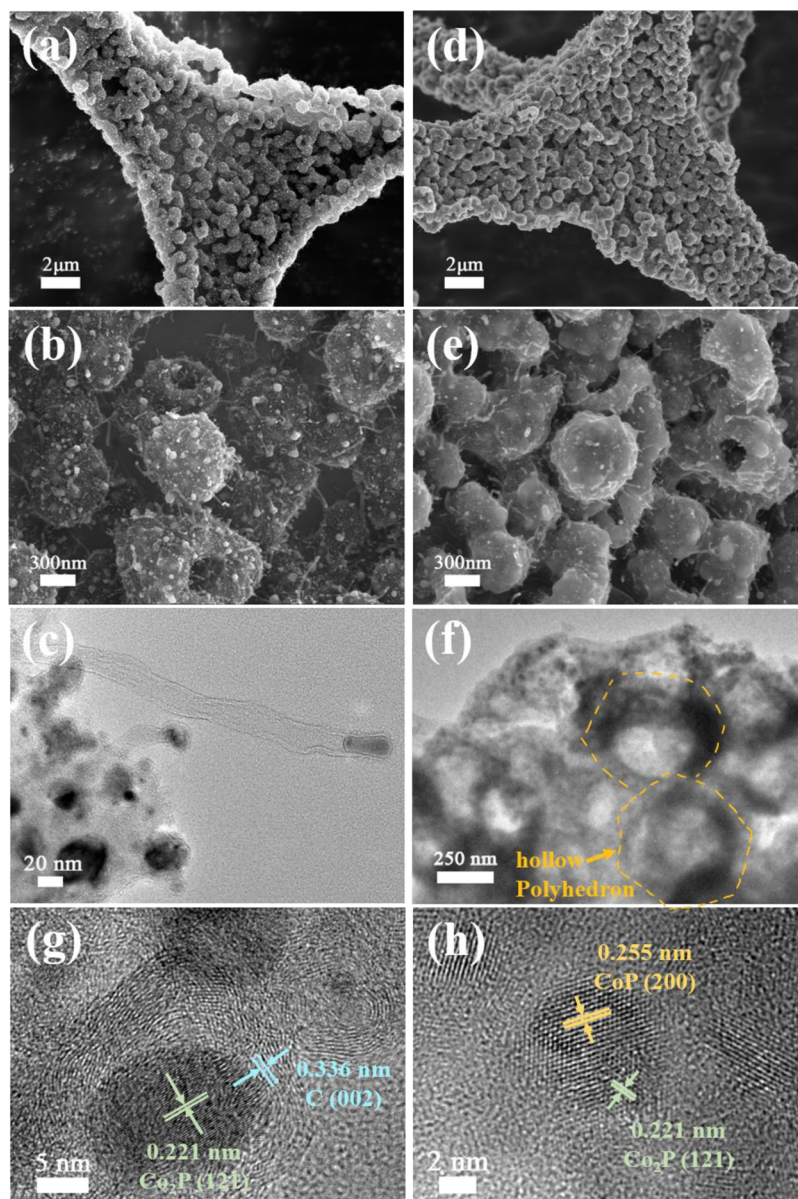
Figure 3. (a,b) SEM images of Co/NCNT@CF, (c) TEM image of Co/CNT, (d,e) SEM images of CoP/Co$_2$P/NCNT@CF, (f) TME image of CoP/Co$_2$P/NCNT@CF, and (g,h) HRTEM images of CoP/Co$_2$P/NCNT@CF.

46.2°, 48.1°, 56.0°, and 56.7° in the XRD spectra of CoP/Co$_2$P/NCNT@CF correspond to the (011), (200), (111), (112), (211), (020), and (301) crystal planes of CoP (JCPDS No. 29-0497), respectively. In addition, the characteristic peak at 40.8° corresponds to the (121) crystal plane of Co$_2$P (JCPDS No.32-0306). This can prove that both CoP and Co$_2$P are present in the phosphating samples. A broader peak at 22° corresponds to the exposed carbon skeleton, and the characteristic peak at 26.3° is the (002) crystal plane of graphitized carbon, which can be attributed to the action of carbon nanotubes.

The microscopic morphology of the as-prepared samples was characterized by scanning electron microscopy (SEM). Figure S2 shows the CF obtained by carbonization of MF at 800 °C in an argon atmosphere, which acts as a conductive carbon skeleton of the entire self-supported catalyst. It can be seen that CF has an interconnected three-dimensional network structure with a flat and smooth skeletal surface. The three-

dimensional network structure is beneficial not only to expose more active sites but also for electron transfer and rapid desorption of hydrogen generated during the reaction process. Figure 3a,b shows the SEM images of Co/NCNT@CF. It can be clearly seen that a layer of hollow polyhedral particles (about 600−700 nm in size) is uniformly attached to the CF backbone, and many carbon nanotubes (length about 100−300 nm) are grown in situ on the inner and outer surfaces of the hollow polyhedron. It can be seen from the TEM image (Figure 3c) of Co/NCNT@CF that the end of each CNT is wrapped with Co nanoparticles (about 20−50 nm). According to previous studies, this is due to the reduction of metallic Co elements by hydrogen, while Co nanoparticles further catalyze the growth of CNT.[9] As shown in Figure 3d,e, the SEM image of CoP/Co$_2$P/NCNT@CF indicates that after phosphating, the hollow polyhedron structure on the CF skeleton is retained, and the metal Co particles distributed on the polyhedral surface are transformed into CoP and Co$_2$P. Figure
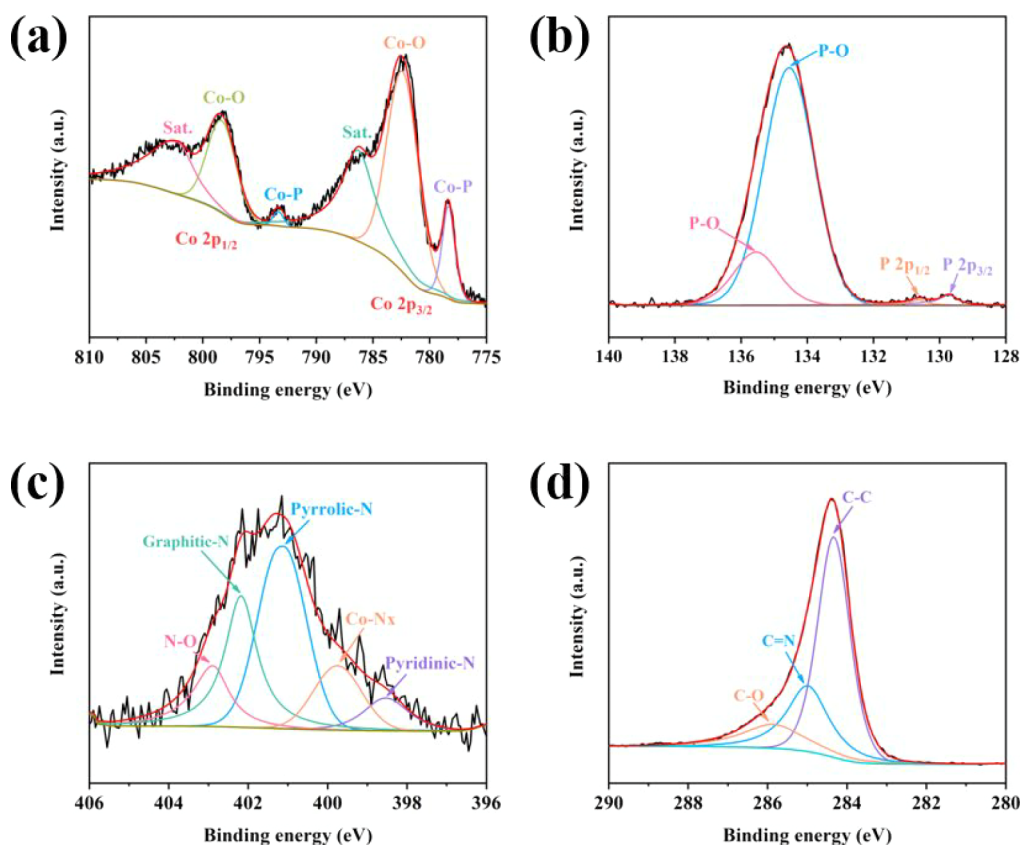
Figure 4. XPS spectra of CoP/Co$_2$P/NCNT@CF: (a) Co 2p, (b) P 2p, (c) N 1s, and (d) C 1s.

3f shows the TEM image of CoP/Co$_2$P/NCNT@CF, which confirms that the polyhedra on the skeleton of CF are hollow structures. In addition, the size of the hollow polyhedron after phosphating shrinks to about 500−600 nm. In addition, the energy spectrum (EDS) recorded in Figure S3 shows that the Co, P, N, and C elements are uniformly distributed on the surface of the catalyst while demonstrating the successful conversion of Co to CoP/Co$_2$P. The microstructural features such as lattice stripes of Co/NCNT@CF were further revealed by HRTEM. HRTEM images of CoP/Co$_2$P/NCNT@CF (Figure 3g,h) show lattice fringes of different widths. The lattice fringes of 0.255 and 0.221 nm correspond to the (200) plane of CoP and the (121) plane of Co$_2$P, respectively, which is consistent with the results of XRD. CoP/Co$_2$P nanoparticles are surrounded by several layers of carbon. The lattice fringe spacing of the carbon layer is about 0.336 nm, corresponding to the (002) plane of C. It is further confirmed that the heterogeneous structure of the CoP/Co$_2$P nanoparticles is embedded in carbon, which is conducive to enhancing the stability of the catalyst in the reaction.

The compositions and chemical states of elements in the samples were investigated by XPS. Figure 4a shows the Co 2p XPS spectra that are attributed to the Co 2p$_{3/2}$ and Co 2p$_{1/2}$ levels due to spin-orbit splitting. The peaks at 778.33, 782.37, and 786.29 eV are attributed to Co 2p$_{3/2}$, while the peaks at 793.35, 798.32, and 802.23 eV are assigned to Co 2p$_{1/2}$. Of these, the binding energies at 778.33 and 793.35 eV correspond to Co−P, thus confirming once again the formation of cobalt phosphide.[45] The binding energies at 782.37 and 798.32 eV are attributed to the oxidized Co species as a result of the surface oxidation of the samples when exposed to air.[46] The peaks at 786.29 and 802.23 eV

correspond to the satellite peaks of Co 2p$_{3/2}$ and Co 2p$_{1/2}$, respectively. The P 2p high-resolution spectrum in Figure 4b shows that the peaks at 129.72 and 130.65 eV are attributed to P 2p$_{3/2}$ and P 2p$_{1/2}$ in cobalt phosphide, respectively. The two peaks at 134.54 and 135.55 eV correspond to P in the oxidation state.[47] The N 1s spectrum (Figure 4c) can be fitted into five subpeaks, which correspond to Pyridinic-N (398.52 eV), Co−Nx (399.75 eV), Pyrrolic-N (401.11 eV), Graphitic-N (402.18 eV), and N−O (402.89 eV), respectively.[48] The presence of Pyrrolic-N and Pyridinic-N can improve the electrocatalytic activity of HER by interacting with H$^+$.[43] The presence of Co-Nx and Co−P peaks indicated the chemical coupling between Co and N or P species, which was beneficial to improve the electrocatalytic activity. In addition, it can be observed that the high-resolution C 1s spectrum (Figure 4d) of CoP/Co$_2$P/NCNT@CF can be deconvoluted into three characteristic peaks corresponding to C−C (284.3 eV), C═N (285 eV), and C−O (285.9 eV).[30] The presence of the C═N bond indicates that nitrogen-doped carbon is indeed formed. As the structure of heteroatom-doped carbon has unique electron distribution, it will promote the adsorption of intermediates on the catalyst surface in the catalytic process and accelerate the electron transfer between the active center and intermediates. Therefore, the structure of nitrogen-doped carbon is very conducive to the improvement of catalytic performance.

3.2. Hydrogen Evolution Reaction (HER) of the Catalyst. The HER performance of the prepared catalyst in N$_2$-saturated alkaline electrolyte solution (1 M KOH, pH = 14) was examined using a standard three-electrode system. For comparison, the bare NF and commercial 20% Pt/C were also tested. Figure 5a shows the LSV curves of all catalysts with a
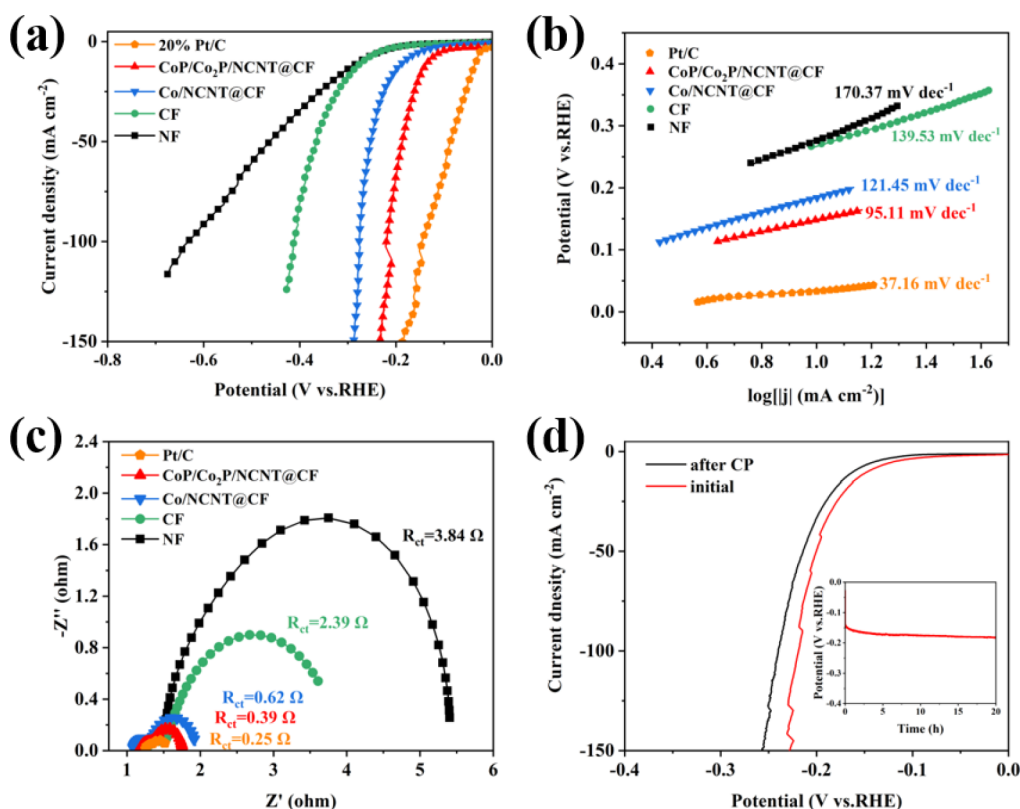
Figure 5. HER performance of the as-prepared samples in N_2-saturated 1.0 M KOH. (a) Polarization curves, (b) corresponding Tafel plots, (c) Nyquist plots with an overpotential of 300 mV vs RHE, and (d) polarization curve of $CoP/Co_2P/NCNT@CF$ before and after 20 h of the chronopotentiometric test (inset: chronopotentiometric response of $CoP/Co_2P/NCNT@CF$ at 10 mA cm^{-2}).

scan rate of 5 mV·s^{-1} at room temperature. As is expected, the 20% Pt/C exhibits a superior HER catalytic activity with a low overpotential of 33 mV to achieve a current density of 10 mA cm^{-2}. Meanwhile, the bare NF has the worst HER performance, requiring an overpotential of 296 mV to reach a current density of 10 mA cm^{-2}. Among the as-prepared electrocatalysts, $CoP/Co_2P/NCNT@CF$ shows a higher HER catalytic activity with an overpotential of 133 mV than Co/NCNT@CF (183 mV) and CF (269 mV) at 10 mA cm^{-2}, which can be attributed to the positive effect of phosphorylation. The abundant Co−P bonds in $CoP/Co_2P/NCNT@CF$ facilitate more proton acceptor sites for HER, and thus, it has a superior HER catalytic activity to other samples.

To evaluate the HER kinetics of the catalyst, the Tafel slope was obtained by fitting the LSV curve. According to previous studies,[49] the occurrence of HER involves three reaction steps. In alkaline solutions, the first step is the Volmer reaction (where the Tafel slope corresponds to 120 mV dec^{-1}), and the second step is the Heyrovsky reaction (where the Tafel slope corresponds to 40 mV dec^{-1}) or the Tafel reaction (where the Tafel slope corresponds to 30 mV dec^{-1}). As shown in Figure 5b, Pt/C still has the smallest Tafel slope of 37.16 mV dec^{-1}, and $CoP/Co_2P/NCNT@CF$ has a lower Tafel slope of 95.11 mV dec^{-1} than the other samples. The Tafel slopes for Co/NCNT@CF, CF, and NF were 121.45, 139.53, and 170.37 mV dec^{-1}, respectively. This result indicates the superior HER kinetic properties for $CoP/Co_2P/NCNT@CF$. $CoP/Co_2P/NCNT@CF$ follows the Volmer−Heyrovsky mechanism, while the other samples follow the Volmer mechanism.

EIS was tested at an overpotential of 300 mV (vs RHE) to further investigate the electrocatalytic kinetics of HER.

According to the Nyquist diagram of its equivalent circuit (Figure 5c), $CoP/Co_2P/NCNT@CF$ has a small charge transfer resistance (R_{ct}) of 0.36 Ω, while the R_{ct} values of Co/NCNT@CF and CF are 0.62 and 2.39 Ω, respectively. The smaller R_{ct} value indicates a strong charge transfer capability and a faster Faraday process, so $CoP/Co_2P/NCNT@CF$ has optimal HER kinetics and the best HER performance.

It is well known that the long-term durability of the catalyst is another important criterion for evaluating electrocatalysts. The $CoP/Co_2P/NCNT@CF$ composite was continuously monitored for 20 h at constant current density (10 mA cm^{-2}) by chronopotentiometry. As shown in Figure 5d, the overpotential of $CoP/Co_2P/NCNT@CF$ increased by 36 mV for the first 10 h of continuous testing, and after 10 h, the overpotential only increased by 7 mV. It is clear that the $CoP/Co_2P/NCNT@CF$ composite maintains its catalytic activity throughout the continuous HER electrocatalytic reaction. This can be attributed to the fact that the catalyst was formed by in situ growth of CoP/NCNT on a CF substrate, and there is strong adhesion between them, so that the prepared self-supported $CoP/Co_2P/NCNT@CF$ catalyst has good long-term stability.

Furthermore, in order to evaluate the electrochemically active surface area, the double-layer capacitance (C_{dl}) of $CoP/Co_2P/NCNT@CF$, Co/NCNT@CF, and CF was calculated by CV curves in the non-Faraday potential range. Figure S4a−c shows the CV plots for different samples at different sweep rates from 10 to 100 mV s^{-1}. The corresponding C_{dl} values are shown in Figure S4d. The C_{dl} values for $CoP/Co_2P/NCNT@CF$, Co/NCNT@CF, and CF are 86.56, 52.49, and 25.54 mF
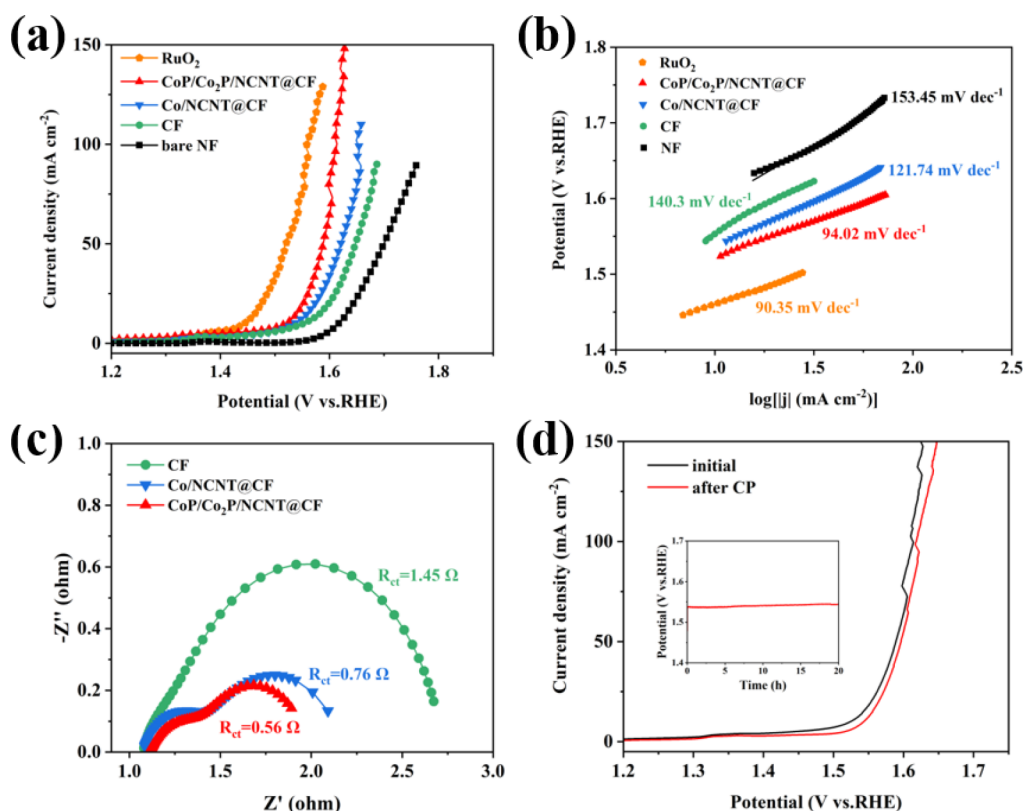
Figure 6. OER performance of the as-prepared samples in O_2-saturated 1.0 M KOH. (a) Polarization curves, (b) corresponding Tafel plots, (c) Nyquist plots with an overpotential of 400 mV vs RHE, (d) polarization curve of CoP/Co$_2$P/NCNT@CF before and after 20 h of the chronopotentiometric test. (Inset: chronopotentiometric response of CoP/Co$_2$P/NCNT@CF at 10 mA·cm^{-2}).

cm^{-2}, respectively. It can be seen that the C_{dl} value of CoP/Co$_2$P/NCNT@CF is about 1.65 times that of Co/NCNT@CF and 3.39 times that of CF, so CoP/Co$_2$P/NCNT@CF has the best catalytic activity.

3.3. Oxygen Evolution Reaction (OER) of the Catalyst.
As the other half reaction of electrocatalytic water cracking, the OER performances of CoP/NCNT and reference samples were investigated in 1 M O_2-saturated KOH solution. Figure 6a presents the OER polarization curves with a scan rate of 5 mV·s^{-1}. As a comparative reference, the OER performances of commercial RuO$_2$ and bare NF were tested, and they required 1.443 and 1.617 V to achieve a current density of 10 mA cm^{-2}, respectively. Among all the prepared samples, CoP/Co$_2$P/NCNT@CF exhibited the lowest overpotential of 1.519 V at 10 mA cm^{-2}, which was superior to Co/NCNT@CF (1.535 V) and CF (1.553 V). At a current density of 50 mA cm^{-2}, the OER performance gap between different samples is more obvious, and CoP/Co$_2$P/NCNT@CF only requires 1.588 V overpotential, while Co/NCNT@CF and CF require 1.62 and 1.647 V, respectively. It is worth noting that only CoP/Co$_2$P/NCNT@CF of all the tested samples could achieve a current density of 150 mA cm^{-2}. The synergy of CoP and Co2P can provide more catalytically active centers for the OER reaction. Co$_2$P in CoP/Co$_2$P/NCNT@CF has a large number of Co–Co bonds, which greatly facilitates the formation of OER active intermediates (OOH*). In summary, CoP/Co$_2$P/NCNT@CF has the best OER performance. In addition, CoP/Co$_2$P/NCNT@CF shows comparable and even superior HER and OER catalytic performance to the recently reported cobalt phosphide-based electrocatalysts in alkaline media (Table S1).

Figure 6b shows the Tafel slope of different samples to evaluate the electrocatalytic kinetics of OER. In line with the LSV results, the corresponding Tafel plot of the catalyst shows that CoP/Co$_2$P/NCNT@CF has a small Tafel slope of 94.02 mV dec^{-1}, which is very close to that of commercial RuO$_2$ (90.35 mV dec^{-1}). The Tafel slopes for Co/NCNT@CF, CF, and NF were 121.74, 140.3, and 153.45 mV dec^{-1}, respectively. The results demonstrate the rapid OER kinetics and high electrocatalytic activity of CoP/Co$_2$P/NCNT@CF.

To gain further insight into the catalytic activity of the catalyst samples, EIS measurements were carried out at an overpotential of 400 mV (vs RHE). Nyquist plots for the different samples are shown in Figure 6c, and CoP/Co$_2$P/NCNT@CF (R_{ct} = 0.26 Ω) has a smaller charge transfer resistance than Co/NCNT@CF (R_{ct} = 0.76 Ω) and CF (R_{ct} = 1.45 Ω). This implies that CoP/Co$_2$P/NCNT@CF has a faster ion transfer rate during OER and therefore has the best OER electrocatalytic activity.

Furthermore, the stability of CoP/Co$_2$P/NCNT@CF during the OER reaction was assessed using the same method as the HER stability test. As shown in Figure 6d, the CoP/Co$_2$P/NCNT@CF composite exhibited excellent stability in alkaline environments. After 20 h of continuous operation at a current density of 10 mA cm^{-2}, the overpotential increased by only 24 mV. By comparing the LSV curves before and after the stability test, it was found that there was only a small difference between the two curves, indicating that there was no significant decay in the catalytic activity of the OER. In summary, CoP/Co$_2$P/NCNT@CF is expected to be an alternative to precious metal-based catalysts in practical applications due to its excellent stability.

4. CONCLUSIONS

In summary, we have successfully prepared a nitrogen-doped carbon nanotube-enhanced 3D self-supported electrocatalyst ($CoP/Co_2P/NCNT@CF$) with a conductive carbon network backbone as the support substrate and the coexistence of CoP and Co_2P by a two-step strategy of high-temperature carbonization and low-temperature phosphorylation. The three-dimensional carbon network backbone of this catalyst provides fast access for mass and charge transfer, while the hollow structure provides a large number of active sites. The strongly coupled $CoP/Co_2P/NCNT@CF$ electrocatalyst exhibits good bifunctional electrocatalytic performance in alkaline environments, requiring only 133 mV and 1.519 V (289 mV) low overpotential to drive HER and OER up to 10 mA cm^{-2}, respectively. In addition, the tight connections between $CoP/Co_2P/NCNTs$ and CF effectively prevent agglomeration, which gives the composite catalyst strong durability. The synthesized electrocatalyst has the advantages of low cost, high activity, and good stability and has great potential in the production of hydrogen and oxygen by large-scale electrolysis of water. This work provides new ideas for the design and development of nonprecious metal catalysts.

■ ASSOCIATED CONTENT

ⓢ Supporting Information

The Supporting Information is available free of charge at https://pubs.acs.org/doi/10.1021/acsomega.2c00123.

> Digital photographs of MF, MF/ZIF, and after carbonization (Figure S1); SEM images of the carbon foam (Figure S2); SEM-EDS analysis of the $CoP/Co_2P/NCNT@CF$ (Figure S3); CV curves and C_{dl} of the samples (Figure S4); equivalent circuit diagram (Figure S5); and performance comparison of cobalt phosphide-based electrocatalysts (Table S1) (PDF)

■ AUTHOR INFORMATION

Corresponding Author

Nannan Wang − *Key Laboratory of New Processing Technology for Nonferrous Metals and Materials, Ministry of Education, School of Resources, Environment and Materials, Guangxi Institute Fullerene Technology (GIFT), Guangxi University, Nanning 530004, China;* ⓞ orcid.org/0000-0002-9013-0612; Email: wangnannan@gxu.edu.cn

Authors

Linyi Zhang − *Key Laboratory of New Processing Technology for Nonferrous Metals and Materials, Ministry of Education, School of Resources, Environment and Materials, Guangxi Institute Fullerene Technology (GIFT), Guangxi University, Nanning 530004, China*

Yu Chen − *College of Engineering, Department of Mathematics and Physical Sciences, University of Exeter, Exeter EX4 4QF, U.K.*

Guangsheng Liu − *Key Laboratory of New Processing Technology for Nonferrous Metals and Materials, Ministry of Education, School of Resources, Environment and Materials, Guangxi Institute Fullerene Technology (GIFT), Guangxi University, Nanning 530004, China*

Zhen Li − *Key Laboratory of New Processing Technology for Nonferrous Metals and Materials, Ministry of Education, School of Resources, Environment and Materials, Guangxi*

Institute Fullerene Technology (GIFT), Guangxi University, Nanning 530004, China

Song Liu − *Key Laboratory of New Processing Technology for Nonferrous Metals and Materials, Ministry of Education, School of Resources, Environment and Materials, Guangxi Institute Fullerene Technology (GIFT), Guangxi University, Nanning 530004, China*

Santosh K. Tiwari − *Key Laboratory of New Processing Technology for Nonferrous Metals and Materials, Ministry of Education, School of Resources, Environment and Materials, Guangxi Institute Fullerene Technology (GIFT), Guangxi University, Nanning 530004, China;* ⓞ orcid.org/0000-0003-1602-9345

Oluwafunmilola Ola − *Advanced Materials Group, Faculty of Engineering, The University of Nottingham, Nottingham NG7 2RD, U.K.*

Bingyan Pang − *Key Laboratory of New Processing Technology for Nonferrous Metals and Materials, Ministry of Education, School of Resources, Environment and Materials, Guangxi Institute Fullerene Technology (GIFT), Guangxi University, Nanning 530004, China*

Yanqiu Zhu − *Key Laboratory of New Processing Technology for Nonferrous Metals and Materials, Ministry of Education, School of Resources, Environment and Materials, Guangxi Institute Fullerene Technology (GIFT), Guangxi University, Nanning 530004, China; College of Engineering, Department of Mathematics and Physical Sciences, University of Exeter, Exeter EX4 4QF, U.K.;* ⓞ orcid.org/0000-0003-3659-5643

Complete contact information is available at:
https://pubs.acs.org/10.1021/acsomega.2c00123

Notes

The authors declare no competing financial interest.

■ ACKNOWLEDGMENTS

■ REFERENCES

(1) Han, N.; Yang, K. R.; Lu, Z.; Li, Y.; Xu, W.; Gao, T.; Cai, Z.; Zhang, Y.; Batista, V. S.; Liu, W.; Sun, X. Nitrogen-doped tungsten carbide nanoarray as an efficient bifunctional electrocatalyst for water splitting in acid. *Nat. Commun.* **2018**, *9*, 924.

(2) Lin, Y.; Sun, K.; Chen, X.; Chen, C.; Pan, Y.; Li, X.; Zhang, J. High-precision regulation synthesis of Fe-doped Co_2P nanorod bundles as efficient electrocatalysts for hydrogen evolution in all-pH range and seawater. *J. Energy Chem.* **2021**, *55*, 92−101.

(3) Cao, Y.; Wang, T.; Li, X.; Zhang, L.; Luo, Y.; Zhang, F.; Asiri, A. M.; Hu, J.; Liu, Q.; Sun, X. A hierarchical CuO@NiCo layered double hydroxide core−shell nanoarray as an efficient electrocatalyst for the oxygen evolution reaction. *Inorg. Chem. Front.* **2021**, *8*, 3049−3054.

(4) Ye, R.; Liu, Y.; Peng, Z.; Wang, T.; Jalilov, A. S.; Yakobson, B. I.; Wei, S. H.; Tour, J. M. High Performance Electrocatalytic Reaction of Hydrogen and Oxygen on Ruthenium Nanoclusters. *ACS Appl. Mater. Interfaces* **2017**, *9*, 3785−3791.

(5) Qiu, Y.; Zhang, X.; Han, H.; Liu, Z.; Liu, J.; Ji, X. Advantageous metal-atom-escape towards super-hydrophilic interfaces assembly for efficient overall water splitting. *J. Power Sources* **2021**, *499*, No. 229941.

(6) Sun, H.; Zhang, W.; Li, J.-G.; Li, Z.; Ao, X.; Xue, K.-H.; Ostrikov, K. K.; Tang, J.; Wang, C. Rh-engineered ultrathin NiFe-LDH nanosheets enable highly-efficient overall water splitting and urea electrolysis. *Appl. Catal., B* **2021**, *284*, No. 119740.

(7) Cao, S.; Liu, Y.; Bo, T.; Xu, R.; Mu, N.; Zhou, W. Prediction of functionalized graphene as potential catalysts for overall water splitting. *Appl. Surf. Sci.* **2022**, *578*, No. 151989.

(8) Ji, L.; Zheng, H.; Wei, Y.; Fang, Y.; Du, J.; Wang, T.; Wang, S. Formation of cobalt phosphide nanodisks as a bifunctional electrocatalyst for enhanced water splitting. *Sustainable Energy Fuels* **2020**, *4*, 1616−1620.

(9) Xia, B. Y.; Yan, Y.; Li, N.; Wu, H. B.; Lou, X. W.; Wang, X. A metal−organic framework-derived bifunctional oxygen electrocatalyst. *Nat. Energy* **2016**, *1*, 15006.

(10) Li, S.; Hao, X.; Abudula, A.; Guan, G. Nanostructured Co-based bifunctional electrocatalysts for energy conversion and storage: current status and perspectives. *J. Mater. Chem. A* **2019**, *7*, 18674−18707.

(11) Liu, J.; Dang, J.; Wang, M.; Wang, X.; Duan, X.; Yuan, S.; Liu, T.; Wang, Q. Metal-Organic-Framework-Derived Cobalt nanoparticles encapsulated in Nitrogen-Doped carbon nanotubes on Ni foam integrated Electrode: Highly electroactive and durable catalysts for overall water splitting. *J. Colloid Interface Sci.* **2022**, *606*, 38−46.

(12) Yang, X.; Li, H.; Lu, A.-Y.; Min, S.; Idriss, Z.; Hedhili, M. N.; Huang, K.-W.; Idriss, H.; Li, L.-J. Highly acid-durable carbon coated Co_3O_4 nanoarrays as efficient oxygen evolution electrocatalysts. *Nano Energy* **2016**, *25*, 42−50.

(13) Zhou, Q.; Li, T.-T.; Qian, J.; Hu, Y.; Guo, F.; Zheng, Y.-Q. Self-supported hierarchical $CuOx@Co_3O_4$ heterostructures as efficient bifunctional electrocatalysts for water splitting. *J. Mater. Chem. A* **2018**, *6*, 14431−14439.

(14) Wang, Z.; Ji, S.; Liu, F.; Wang, H.; Wang, X.; Wang, Q.; Pollet, B. G.; Wang, R. Highly Efficient and Stable Catalyst Based on $Co(OH)_2@Ni$ Electroplated on Cu-Metallized Cotton Textile for Water Splitting. *ACS Appl. Mater. Interfaces* **2019**, *11*, 29791−29798.

(15) Zhou, X.; Yang, X.; Hedhili, M. N.; Li, H.; Min, S.; Ming, J.; Huang, K.-W.; Zhang, W.; Li, L.-J. Symmetrical synergy of hybrid Co_9S_8-MoS_x electrocatalysts for hydrogen evolution reaction. *Nano Energy* **2017**, *32*, 470−478.

(16) Yan, L.; Wang, H.; Shen, J.; Ning, J.; Zhong, Y.; Hu, Y. Formation of mesoporous Co/CoS/Metal-N-C@S, N-codoped hairy carbon polyhedrons as an efficient trifunctional electrocatalyst for Zn-air batteries and water splitting. *Chem. Eng. J.* **2021**, *403*, No. 126385.

(17) Liu, T.; Li, P.; Yao, N.; Cheng, G.; Chen, S.; Luo, W.; Yin, Y. CoP-Doped MOF-Based Electrocatalyst for pH-Universal Hydrogen Evolution Reaction. *Angew. Chem., Int. Ed. Engl.* **2019**, *58*, 4679−4684.

(18) Liu, G.; Wang, M.; Xu, Y.; Wang, X.; Li, X.; Liu, J.; Cui, X.; Jiang, L. Porous CoP/Co_2P heterostructure for efficient hydrogen evolution and application in magnesium/seawater battery. *J. Power Sources* **2021**, *486*, No. 229351.

(19) Xu, M.; Han, L.; Han, Y.; Yu, Y.; Zhai, J.; Dong, S. Porous CoP concave polyhedron electrocatalysts synthesized from metal−organic frameworks with enhanced electrochemical properties for hydrogen evolution. *J. Mater. Chem. A* **2015**, *3*, 21471−21477.

(20) Wang, P.; Zhu, J.; Pu, Z.; Qin, R.; Zhang, C.; Chen, D.; Liu, Q.; Wu, D.; Li, W.; Liu, S.; Xiao, J.; Mu, S. Interfacial engineering of Co nanoparticles/Co_2C nanowires boosts overall water splitting kinetics. *Appl. Catal., B* **2021**, *296*, No. 120334.

(21) Jiang, J.; Liu, Q.; Zeng, C.; Ai, L. Cobalt/molybdenum carbide@N-doped carbon as a bifunctional electrocatalyst for hydrogen and oxygen evolution reactions. *J. Mater. Chem. A* **2017**, *5*, 16929−16935.

(22) Ray, C.; Lee, S. C.; Jin, B.; Kundu, A.; Park, J. H.; Chan Jun, S. Conceptual design of three-dimensional CoN/Ni_3N-coupled nanograsses integrated on N-doped carbon to serve as efficient and robust water splitting electrocatalysts. *J. Mater. Chem. A* **2018**, *6*, 4466−4476.

(23) Zhang, M.; Ci, S.; Li, H.; Cai, P.; Xu, H.; Wen, Z. Highly defective porous CoP nanowire as electrocatalyst for full water splitting. *Int. J. Hydrogen Energy* **2017**, *42*, 29080−29090.

(24) Zhang, B.; Li, C.; Hu, J.; Peng, D.; Huang, K.; Wu, J.; Chen, Z.; Huang, Y. Cobalt tungsten phosphide with tunable W-doping as highly efficient electrocatalysts for hydrogen evolution reaction. *Nano Res.* **2021**, *14*, 4073−4078.

(25) Liu, Y.; Zhu, Y.; Shen, J.; Huang, J.; Yang, X.; Li, C. CoP nanoparticles anchored on N,P-dual-doped graphene-like carbon as a catalyst for water splitting in non-acidic media. *Nanoscale* **2018**, *10*, 2603−2612.

(26) Yang, D.; Hou, W.; Lu, Y.; Zhang, W.; Chen, Y. Cobalt phosphide nanoparticles supported within network of N-doped carbon nanotubes as a multifunctional and scalable electrocatalyst for water splitting. *J. Energy Chem.* **2021**, *52*, 130−138.

(27) Hou, C. C.; Cao, S.; Fu, W. F.; Chen, Y. Ultrafine CoP Nanoparticles Supported on Carbon Nanotubes as Highly Active Electrocatalyst for Both Oxygen and Hydrogen Evolution in Basic Media. *ACS Appl. Mater. Interfaces* **2015**, *7*, 28412−28419.

(28) Yan, L.; Zhang, B.; Zhu, J.; Liu, Z.; Zhang, H.; Li, Y. Callistemon-like Zn and S codoped CoP nanorod clusters as highly efficient electrocatalysts for neutral-pH overall water splitting. *J. Mater. Chem. A* **2019**, *7*, 22453−22462.

(29) Liu, T.; Xie, L.; Yang, J.; Kong, R.; Du, G.; Asiri, A. M.; Sun, X.; Chen, L. Self-Standing CoP Nanosheets Array: A Three-Dimensional Bifunctional Catalyst Electrode for Overall Water Splitting in both Neutral and Alkaline Media. *ChemElectroChem* **2017**, *4*, 1840−1845.

(30) Tong, J.; Li, Y.; Bo, L.; Li, W.; Li, T.; Zhang, Q.; Kong, D.; Wang, H.; Li, C. CoP/N-Doped Carbon Hollow Spheres Anchored on Electrospinning Core−Shell N-Doped Carbon Nanofibers as Efficient Electrocatalysts for Water Splitting. *ACS Sustainable Chem. Eng.* **2019**, *7*, 17432−17442.

(31) Xie, X.-Q.; Liu, J.; Gu, C.; Li, J.; Zhao, Y.; Liu, C.-S. Hierarchical structured CoP nanosheets/carbon nanofibers bifunctional eletrocatalyst for high-efficient overall water splitting. *J. Energy Chem.* **2022**, *64*, 503−510.

(32) Qiu, Y.; Jia, Q.; Yan, S.; Liu, B.; Liu, J.; Ji, X. Favorable Amorphous-Crystalline Iron Oxyhydroxide Phase Boundaries for Boosted Alkaline Water Oxidation. *ChemSusChem* **2020**, *13*, 4911−4915.

(33) Qiu, Y.; Zhou, J.; Liu, Z.; Zhang, X.; Han, H.; Ji, X.; Liu, J. Solar-driven photoelectron injection effect on $MgCo_2O_4@WO_3$ core−shell heterostructure for efficient overall water splitting. *Appl. Surf. Sci.* **2022**, *578*, No. 152049.

(34) Xu, H.; Shang, H.; Wang, C.; Du, Y. Surface and interface engineering of noble-metal-free electrocatalysts for efficient overall water splitting. *Coord. Chem. Rev.* **2020**, *418*, No. 213374.

(35) Li, H.; Li, Q.; Wen, P.; Williams, T. B.; Adhikari, S.; Dun, C.; Lu, C.; Itanze, D.; Jiang, L.; Carroll, D. L.; Donati, G. L.; Lundin, P. M.; Qiu, Y.; Geyer, S. M. Colloidal Cobalt Phosphide Nanocrystals as Trifunctional Electrocatalysts for Overall Water Splitting Powered by a Zinc-Air Battery. *Adv. Mater.* **2018**, *30*, No. 1705796.

(36) Qiu, Y.; Liu, Z.; Zhang, X.; Sun, A.; Ji, X.; Liu, J. Controllable atom implantation for achieving Coulomb-force unbalance toward lattice distortion and vacancy construction for accelerated water splitting. *J. Colloid Interface Sci.* **2022**, *610*, 194−201.

(37) Sun, C.; Dong, Q.; Yang, J.; Dai, Z.; Lin, J.; Chen, P.; Huang, W.; Dong, X. Metal−organic framework derived $CoSe_2$ nanoparticles anchored on carbon fibers as bifunctional electrocatalysts for efficient overall water splitting. *Nano Res.* **2016**, *9*, 2234−2243.

(38) Andrew Lin, K.-Y.; Chang, H.-A. A zeolitic imidazole framework (ZIF)−sponge composite prepared via a surfactant-assisted dip-coating method. *J. Mater. Chem. A* **2015**, *3*, 20060−20064.

(39) Zhu, H.; Zhang, Q.; Li, B.-G.; Zhu, S. Engineering Elastic ZIF-8-Sponges for Oil-Water Separation. *Adv. Mater. Interfaces* **2017**, *4*, No. 1700560.

(40) Lei, Z.; Deng, Y.; Wang, C. Multiphase surface growth of hydrophobic ZIF-8 on melamine sponge for excellent oil/water

separation and effective catalysis in a Knoevenagel reaction. *J. Mater. Chem. A* **2018**, *6*, 3258−3263.

(41) Yang, X.; Tang, Q.; Jiang, Y.; Zhang, M.; Wang, M.; Mao, L. Nanoscale ATP-Responsive Zeolitic Imidazole Framework-90 as a General Platform for Cytosolic Protein Delivery and Genome Editing. *J. Am. Chem. Soc.* **2019**, *141*, 3782−3786.

(42) You, B.; Jiang, N.; Sheng, M.; Gul, S.; Yano, J.; Sun, Y. High-Performance Overall Water Splitting Electrocatalysts Derived from Cobalt-Based Metal−Organic Frameworks. *Chem. Mater.* **2015**, *27*, 7636−7642.

(43) Pan, Y.; Sun, K.; Liu, S.; Cao, X.; Wu, K.; Cheong, W. C.; Chen, Z.; Wang, Y.; Li, Y.; Liu, Y.; Wang, D.; Peng, Q.; Chen, C.; Li, Y. Core-Shell ZIF-8@ZIF-67-Derived CoP Nanoparticle-Embedded N-Doped Carbon Nanotube Hollow Polyhedron for Efficient Overall Water Splitting. *J. Am. Chem. Soc.* **2018**, *140*, 2610−2618.

(44) Chen, Z.; Ha, Y.; Jia, H.; Yan, X.; Chen, M.; Liu, M.; Wu, R. Oriented Transformation of Co-LDH into 2D/3D ZIF-67 to Achieve Co−N−C Hybrids for Efficient Overall Water Splitting. *Adv. Energy Mater.* **2019**, *9*, No. 1970066.

(45) Lu, Y.; Deng, Y.; Lu, S.; Liu, Y.; Lang, J.; Cao, X.; Gu, H. MOF-derived cobalt-nickel phosphide nanoboxes as electrocatalysts for the hydrogen evolution reaction. *Nanoscale* **2019**, *11*, 21259−21265.

(46) Shi, J.; Qiu, F.; Yuan, W.; Guo, M.; Lu, Z.-H. Nitrogen-doped carbon-decorated yolk-shell CoP@FeCoP micro-polyhedra derived from MOF for efficient overall water splitting. *Chem. Eng. J.* **2021**, *403*, No. 126312.

(47) Zhang, X.; Zhang, L.; Xu, G.; Zhao, A.; Zhang, S.; Zhao, T.; Jia, D. Template Construction of Porous CoP/COP$_2$ Microflowers Threaded with Carbon Nanotubes toward High-Efficiency Oxygen Evolution and Hydrogen Evolution Electrocatalysts. *Inorg. Chem.* **2020**, *59*, 12232−12239.

(48) Guo, Y.; Yuan, P.; Zhang, J.; Xia, H.; Cheng, F.; Zhou, M.; Li, J.; Qiao, Y.; Mu, S.; Xu, Q. Co$_2$ P-CoN Double Active Centers Confined in N-Doped Carbon Nanotube: Heterostructural Engineering for Trifunctional Catalysis toward HER, ORR, OER, and Zn-Air Batteries Driven Water Splitting. *Adv. Funct. Mater.* **2018**, *28*, No. 1805641.

(49) Ali, A.; Shen, P. K. Nonprecious metal's graphene-supported electrocatalysts for hydrogen evolution reaction: Fundamentals to applications. *Carbon Energy* **2019**, *2*, 99−121.